Journal of the European Ceramic Society 18 (1998) 1187–1194

PII: S0955-2219(98)0041-7
0955-2219/98/$—see front matter

Thermal Behaviour of SiCN Nanopowders Issued from Laser Pyrolysis

M. Mayne,[a] D. Bahloul-Hourlier,[a]* B. Doucey,[a] P. Goursat,[a] M. Cauchetier[b] and N. Herlin[b]

[a]LMCTS, UPRES-A 6015, 123 Avenue A. Thomas, 87060 Limoges Cedex, France
[b]CEA-DRECAM-SPAM, CE Saclay, 91191 Gif sur Yvette Cedex, France

Abstract

The thermal behaviour of two SiCN nanopowders (C/N=0·87 and C/N=0·22), issued from laser pyrolysis, is studied under two different atmospheres (He, N_2) by means of thermogravimetry coupled with mass spectrometry, and X-ray diffraction. In the 25–1200°C temperature range, the same behaviour in both helium and nitrogen is observed for the two SiCN nanopowders: very little weight loss occurs because of the evolution of adsorbed water, residual synthesis gases and also methane, hydrogen and carbon monoxide. However, above 1200°C, the significant weight loss associated with the release of nitrogen and oxide species, under helium, is related to the decomposition process; whereas under nitrogen the weight gain results from the nitriding process. These two phenomena are more important for an amorphous powder. A comparison of the hot-pressing of Si_3N_4 UBE and SiCN nanopowders with sintering aids (Y_2O_3, Al_2O_3) indicates that the α to β Si_3N_4 transformation rate is increased by the small grain size and by the presence of SiC in SiCN nanopowders.© 1998 Elsevier Science Limited. All rights reserved

Le comportement thermique de deux nanopoudres SiCN (C/N=0·87 et C/N=0·22), synthétisées par pyrolyse laser, est étudié par thermogravimétrie couplée à l'analyse de gaz par spectrométrie de masse sous atmosphère inerte (He) ou réactive (N_2). Dans le domaine de température compris entre 25 et 1200°C, le même comportement, à la fois sous hélium et sous azote, est observé pour les deux poudres SiCN : la faible perte de masse provient des dégagements d'eau adsorbée, de gaz résiduels de synthèse, ainsi que de méthane, d'hydrogène et de monoxyde de carbone. En revanche, à partir de 1200°C, sous hélium, l'importante perte de masse accompagnée des dégagements d'azote et de composés oxygénés, est liée à la décomposition des poudres; alors que sous azote le gain de masse résulte d'un processus de nitruration. Ces deux phénomènes sont d'autant plus importants que la poudre est amorphe.Le frittage sous charge de la poudre Si_3N_4 UBE et des nanopoudres SiCN en présence d'ajouts (Y_2O_3, Al_2O_3) met en évidence des taux de transformation Si_3N_4 α → β élevés dans les nanopoudres SiCN en raison de la faible taille des grains et de la présence de SiC. © 1998 Elsevier Science Limited. All rights reserved

1 Introduction

In recent years, much interest has been focused on nanophase materials which, due to their small grain size, can offer improved properties compared to traditional materials.[1,2] Nanocomposite materials containing at least one component having nanometric dimensions, exhibit dramatic improvements in mechanical properties, as has been reported, particularly by Japanese researchers, for Si_3N_4 based nanocomposites.[3–6] Moreover, a further advantage of these systems is their ability to be hot-formed because of their fine microstructures.[7]

In this context, Si_3N_4/SiC(N) nanocomposites are produced in order to fabricate ceramic parts by hot-forming. The approach of the study consists of introducing SiC(N) nanoparticles obtained from laser pyrolysis as a second phase, so as to influence the microstructural development of materials.

The aim of the present work is to determine, on the one hand, the thermal behaviour of SiCN nanopowders in two different atmospheres, and on the other hand, the reactivity of these powders with sintering aids (Y_2O_3, Al_2O_3) compared with the

*To whom correspondence should be addressed.

Si_3N_4 powder constituting the matrix of the nanocomposites. This is necessary to understand the behaviour of the nanometric second phase during the sintering process of nanomaterials.

2 Experimental Procedure

Silicon carbonitride powders are synthesized by a CO_2 laser driven gas phase reaction involving SiH_4, CH_3NH_2 and NH_3 gaseous mixtures (synthesis is carried out at CEA - DRECAM - SPAM, Saclay, France). The experimental apparatus has been described elsewhere.[8] The beam of a continuous wave CO_2 laser enters horizontally the reaction cell through a KCl window and crosses the vertical gaseous flow of reactants injected through an inlet capillary. The reaction is caused by the resonance between the emission of the laser at 10·6 μm and an infrared absorption band of SiH_4. During the process, reactant gases are heated by the absorption of CO_2 laser radiation and decompose, causing particles to nucleate and grow rapidly. An argon flow prevents powder deposition and guides the obtained products into a powder collector. The as-synthesized powders are stored in a glove-box to avoid contamination by air or water vapour.

The main synthesis parameters and chemical composition of the two SiCN nanopowders are reported in Table 1. The chemical composition has been calculated from elemental analysis realized by ICP (Inductive Coupled Plasma) at CNRS (Service Central d'Analyses, Vernaison, France). The well-crystallised compounds (Si_3N_4, SiC...) does not define exactly the SiCN nanopowders. In fact, it has been observed by XPS, EXAFS and XANES that SiCN nanopowders obtained by laser pyrolysis are composed of mixed tetrahedra SiC_xN_{4-x} with a small amount of Si–O bonds.[9–11] The IR spectroscopy study of the surface of SiCN laser synthesized powders shows the presence of Si–OH and Si–H bonds.[8] Moreover, it must be noticed that X-ray diffraction analysis indicates a more pronounced degree of crystallisation in the SiCN29 nanosized powder rich in silicon nitride than in SiCN35 powder.

The thermal behaviour of SiCN nanopowders in flowing helium or nitrogen (flow rate: 25 cm^3 min^{-1}, purity: 99·9999%) is investigated by using a thermogravimetric analyser (Netzsch STA 409) interfaced with a quadrupole mass spectrometer (MS, Quadrex 200, Leybold Heraeus, 70 eV electron impact). This equipment (TG/MS) allows the different gases evolved during the pyrolysis to be identified, and the signals of characteristic ions to be plotted as a function of the temperature along with the TG curve.

Powder samples are preliminary compacted and broken into small parts in order to prevent the suction of fine particles during the vacuum pumping. They are then heated in an alumina crucible from room temperature to 1500°C (for 1 h) with a heating rate of 10°C min^{-1}.

The reactivity of SiCN nanopowders with sintering aids is studied by comparing the α (equiaxed grains) to β (acicular grains) Si_3N_4 phase transformation in SiCN nanopowders and in Si_3N_4 (UBE Industry) powder. Treatments of each powder mixed with sintering aids (Y_2O_3: 6 wt%, Al_2O_3: 3 wt%) at 1530°C for 2 h are carried out by hot-pressing (LPA 200 LC device) in a BN coated graphite die under a constant applied load of 35 MPa in a nitrogen atmosphere.

Phase analysis is carried out by X-ray diffraction with a Philips PW 1130 apparatus equipped with a copper anticathode. Semi quantitative and comparative determination of the weight fraction of α and β Si_3N_4 phases has been made on powder samples before and after heat treatment by using the integrated intensity ratio of the peak [200] for β Si_3N_4 and [201] for α Si_3N_4 corrected according to the calculated calibration curve developed by Gazzara and Messier.[12] The main goal is to estimate the effects of the two different atmospheres and of sintering aids on the α and β Si_3N_4 phase development rather than to measure very precisely the α and β phase content.

3 Results and Discussion

3.1 Thermal behaviour under helium atmosphere

TG studies under a helium flow (Fig. 1) reveal a weight loss which is more important for SiCN35 (−8%) than for SiCN29 nanopowder (−5%). Correlation of the mass spectrometry (MS) results [Figs 2(a) and (b)] with the TG profile indicates that the weight loss occurs in three steps:

- from 25 to 400°C, a small mass fraction is lost, reaching 0·7% for SiCN35 compared with 0·3% for SiCN29 nanopowder. In this temperature range, an evolution of adsorbed

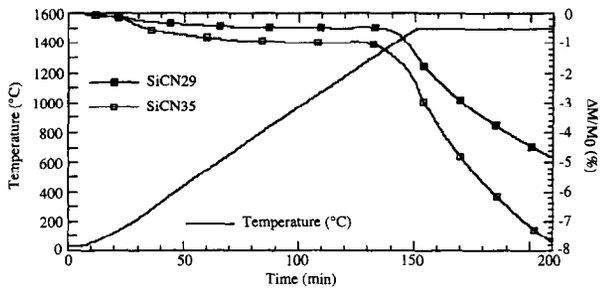

Fig. 1. TG profiles of SiCN nanopowders under helium flow.

Table 1. Synthesis conditions and chemical composition of SiCN nanopowders

Powder grade	*Reactant gas flow rates ($cm^3\ min^{-1}$)*			*Laser power (W)*	*Chemical composition (wt%)*					*C/N atomic ratio*
	SiH_4	*CH_3NH_2*	*NH_3*		*Si_3N_4*	*SiO_2*	*SiC*	*C*	*Si*	
SiCN29	360	90	320	400	86·3	1·1	8·6	4	0	0·22
SiCN35	350	197	0	600	45·1	4·3	45·1	0	5·5	0·87

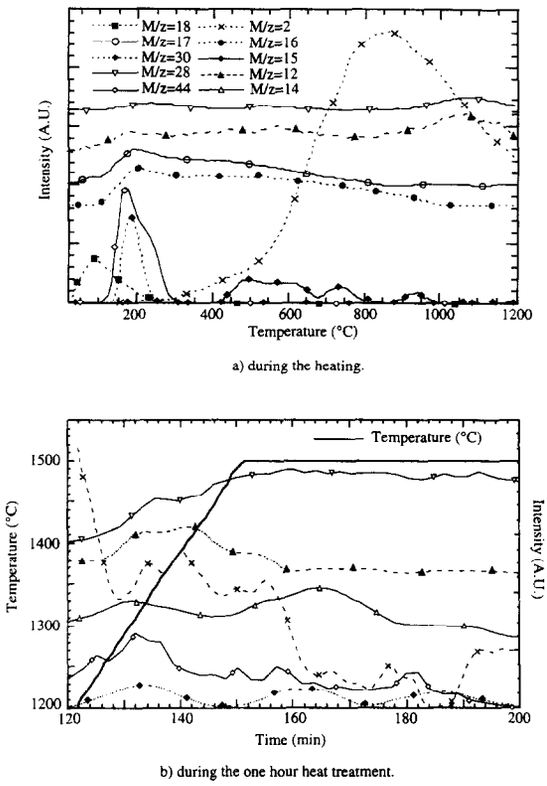

Fig. 2. Gas evolution (MS) during the heat treatment under helium of SiCN35 nanopowder (a) during the heating, (b) during the 1 h heat treatment.

water (H_2O, $m/z=18$, 17) and residual synthesis gases such as NH_3 ($m/z=17$, 16), SiH_4 ($m/z=30$), CH_3NH_2 ($m/z=30$, 28) and CH_3SiH_3 ($m/z=44$) is detected by MS. Whatever the powder, the water release is observed at around 100°C, while the synthesis gases evolve at different temperatures depending on the composition of the powder (SiCN35: 200°C for all synthesis gases compared to SiCN29: 300°C for NH_3 and 400°C for SiH_4 and CH_3NH_2);

- between 400 and 1200°C, the weight loss is very limited in magnitude (i.e.−0·3% in the case of SiCN35, and −0·2% for SiCN29). At the same time an evolution of hydrogen (H_2, $m/z=2$), methane (CH_4, $m/z=16$, 15) and carbon monoxide (CO, $m/z=28$, 12) appears. The evolution of carbon monoxide is maximum around 1100°C for the two powders, unlike methane and hydrogen which evolve, respectively, at 600 and 850°C for SiCN35 and at 750 and 1200°C for SiCN29;
- from 1200 to 1500°C, the most important weight loss is observed. After a 1 h heat treatment at 1500°C, this reaches 6·7% for SiCN35 compared to 4·3% for SiCN29 nanopowder. In this stage, the main gases detected by MS are nitrogen (N_2, $m/z=28$, 14), nitrous oxide (N_2O, $m/z=44$, 30) and carbon monoxide. These gaseous evolutions are maximum around 1350°C for SiCN35 nanopowder, while they evolve at 1500°C for SiCN29. The evolution of such gases takes place during the isothermal treatment (1 h at 1500°C).

3.2 Thermal behaviour under nitrogen atmosphere

TG curves (Fig. 3) of the two treated powders, under nitrogen atmosphere, exhibit similar behaviour and show a weight gain, in particular for SiCN35 nanopowder. Three stages, which are confirmed by MS analysis, may be distinguished. The two first steps (from 25 to 400°C and between 400 and 1200°C) are similar to those obtained under a helium atmosphere, and the same gases are evolved. The third stage (from 1200 to 1500°C) concerns the weight gain, which is higher for SiCN35 (+ 8%) than for SiCN29 nanopowder (+ 0·5%). At the same time, gaseous products detected by MS [Fig. 4(a) and (b)] are carbon monoxide and nitrogen oxides (N_2O, NO $m/z=30$). The evolution of such gases reaches a maximum at 1420°C for SiCN35 nanopowder, while they evolve at around 1500°C for SiCN29.

3.3 X-ray diffraction analysis

Figures 5(a) and (b) compare the XRD patterns of SiCN29 and SiCN35 samples before and after annealing at 1500°C for 1 h, under helium and

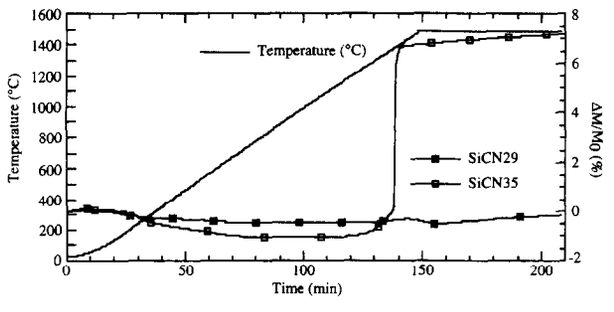

Fig. 3. TG profiles of SiCN nanopowders under nitrogen flow.

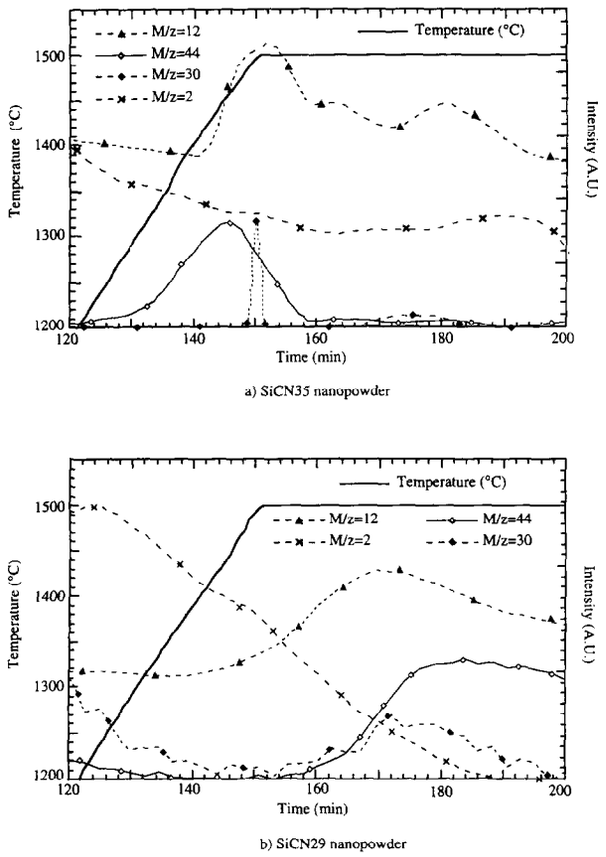

Fig. 4. Gas evolution (MS) during the heat treatment under nitrogen of SICN nanopowders (a) SiCN35, (b) SiCN29 nanopowders.

nitrogen. The development of crystallinity is observed in heat treated samples, particularly for SiCN35 nanopowder [Fig. 5(a)]. Whatever the powder and the nature of the atmosphere, common crystalline phases are observed in annealed samples: α and β Si_3N_4, β SiC (based on JCPDS cards nos 410360, 331160, 291129, respectively). Note that β SiC is difficult to detect in SiCN29 powder because of its low content and the superposition of its specific peaks with those of Si_3N_4.

It is worthy of note that the helium atmosphere yields to the formation of free silicon (JCPDS card no: 271402), especially for SiCN29 nanopowder. For SiCN35, the silicon peak, initially present becomes higher and sharper by annealing the powder under this atmosphere.

Powders treated under nitrogen atmosphere do not contain free silicon. In the case of SiCN35 nanopowder, it must be noticed that the silicon disappears, compared to the as-synthesized powder.

The determination of α or β Si_3N_4 content in annealed powders indicates that a helium atmosphere involves the preferential formation of the β phase, while a nitrogen atmosphere leads preferentially to the α phase. Indeed, after a one hour heat treatment under nitrogen, the content of α Si_3N_4 is 82 wt% for SiCN35 nanopowder and 50 wt% for SiCN29, compared respectively, to 50 wt% and 40 wt% after a 1 h heat treatment under helium atmosphere. Note that the α Si_3N_4 content is approximately the same in the SiCN29 powder treated under nitrogen (50 wt%) as in the as-synthesized powder (47 wt%).

3.4 Reactivity of powders with sintering aids

The α to β Si_3N_4 transformation rate is calculated by comparing the α/β Si_3N_4 content ratio measured by XRD on hot-pressed samples with that measured on as-synthesized powders. Note that such a calculation is only feasible for crystallised powders (SiCN29, Si_3N_4) where α/β initial ratios can be determined ($\alpha/\beta = 100/0$ for Si_3N_4, $\alpha/\beta = 47/53$ for SiCN29). In the case of the semi-crystallised powder (SiCN35), the α/β ratio in the initial powder is extrapolated to that obtained from the crystallised powder under nitrogen atmosphere ($\alpha/\beta = 18/82$). Such an approximation can be made because previous results[13] have indicated that, whatever the SiCN nanopowder, treatments under nitrogen atmosphere without sintering aids in the hot-pressing device at 1530°C for 2 h involve the same α/β ratios as those obtained from heat treatment under nitrogen at 1500°C for 1 h in the TG device.

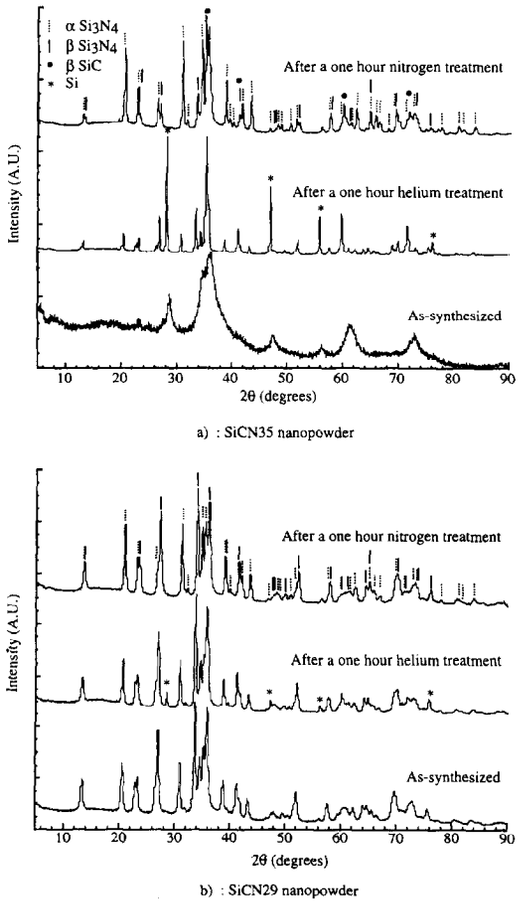

Fig. 5. X-ray diffraction patterns of as-synthesized and heat treated SiCN nanopowders (a) SiCN35, (b) SiCN29 nanopowders.

Results concerning α/β ratios and α to β transformation rates as well as the densification rates of the hot-pressed products are reported in Table 2.

The transformation rate is greater in SiCN nanopowders than in Si_3N_4 powder, suggesting that the ultrafine powders are more reactive with the oxynitride liquid phase formed from the additives (Y_2O_3, Al_2O_3) during sintering.

Moreover low densification rates are observed for SiC enriched nanopowder (SiCN35). In order to compare the reactivity of the two nanopowders in the presence of sintering aids, transformation rates should be weighted by the shrinkage resulting from sintering, because these two parameters play an important role in the densification process. Thus, the β content/shrinkage ratio is equal to 2 for SiCN29 nanopowder compared to 3·2 for SiCN35. Such a result reveals that a high SiC content (SiCN35) induces an important transformation rate.

3.5 Discussion

All these results give evidence of the important reactivity of SiCN nanopowders under different atmospheres and with sintering aids, which varies with the chemical composition and the degree of crystallisation of the powders.

3.5.1 Thermal behaviour of SiCN nanopowders under helium and nitrogen atmospheres

Whatever the powder and the nature of the atmosphere, in the 25–1200°C temperature range, the slight decomposition of powders is explained on the one hand, by the desorption of water, ammonia and gaseous products issued from the synthesis process (CH_3NH_2, SiH_4, CH_3SiH_3), and on the other hand by the evolution of methane, hydrogen and carbon monoxide. Such phenomena have also been observed in the case of SiCN nanopowders obtained by laser spray pyrolysis of liquid precursors,[14] and should arise from the gaseous precursors adsorbed on the surface of powders because of their high specific area ($50\,m^2\,g^{-1}$) and of the quenching during the synthesis process.

Below 400°C, the NH_3 evolution can be explained by transamination–condensation reaction (1, 2). This reaction is equivalent to an exchange of N–Si and N–H bonds[15] (which presence has been demonstrated by IR spectroscopy on the same systems[8]), thus involving the formation of new Si–N bonds which leads to trisilylated nitrogen atoms. Such a reaction has also been reported in studies concerning the polysilazane decomposition.[16]

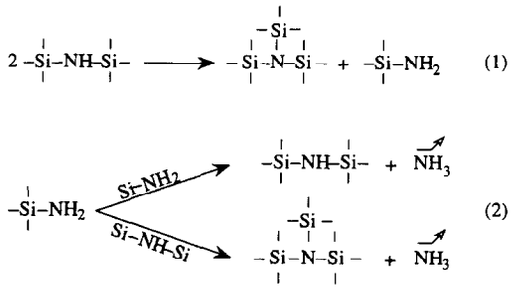

Between 400 and 1200°C, the decomposition reactions most probably involves radical mechanisms.[17,18] The formation of methane arises from radical cleavage of $Si–CH_3$ bonds followed by H abstraction:

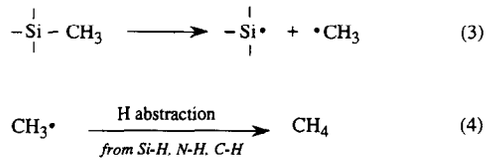

The large escape of hydrogen is due to homolytic cleavage of Si–H, N–H and C–H bonds followed by H abstraction:

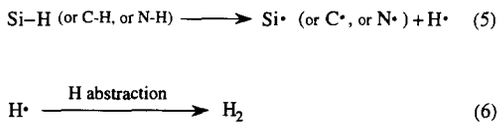

However above 1200°C, the chemical composition and the structural arrangement of SiCN nanopowders depends on the nature of the atmosphere. Under inert atmosphere (He), the important weight loss with the evolution of nitrogen, nitrous oxide and carbon monoxide indicates the decomposition of SiCN(O) phases. Such a weight loss under an inert atmosphere has also been observed for laser SiCN nanopowders issued from liquid precursors.[14] The decomposition phenomenon, previously demonstrated in same systems derived from organometallic precursors,[19] arises from reaction (7). This reaction proceeds by the vapor–liquid–solid (VLS) mechanism involving the formation of a byproduct $Si_{(SLV)}$.

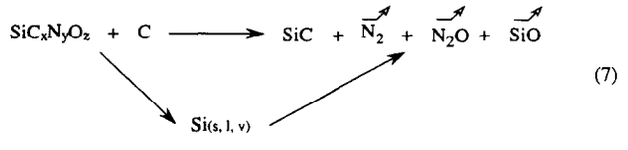

Table 2. Comparison of the α to β Si_3N_4 transformation rate in SiCN nanopowders and in Si_3N_4 UBE powder

Powder grade	*α/β ratio (wt%)*	*$\alpha \rightarrow \beta$ transformation rate (wt%)*	*Densification rate (%)*
Si_3N_4 UBE	70/30	30	
SiCN29	0/100	100	90
SiCN35	20/80	(74)	63

When the free carbon content is low, the SiC formation becomes difficult or impossible. Thus, the evaporation of silicon, depending on the powder bed depth,[19] explains both the weight loss and the formation of free silicon (detected by XRD) in the two SiCN nanopowders treated under helium atmosphere.

In the particular case of a crystallised system containing a large quantity of silicon nitride (SiCN29), reaction (7) is minor and the decomposition phenomenon could be explained by the decomposition reaction of silicon nitride (8).[20] Such a reaction is possible because of the small particle size involving an important reactivity of the Si_3N_4 phase present in SiCN29, and is confirmed by the formation of free silicon (XRD) in SiCN29 treated under helium.

$$Si_3N_4 \longrightarrow 3Si + 2\overrightarrow{N_2} \quad (8)$$

Because of oxygen contamination of the nanopowders (Si–O bonds), active oxidation phenomena of silicon nitride[21,22] can also lead to the decomposition of SiCN29 powder in the 1500°C temperature range, and reactions (9, 10) could be summarised by:

$$Si_3N_4 + 3SiO_2 \longrightarrow 6\overrightarrow{SiO} + 2\overrightarrow{N_2} \quad (9)$$

$$Si_3N_4 + 3/2\,O_2 \longrightarrow 3\overrightarrow{SiO} + 2\overrightarrow{N_2} \quad (10)$$

Note that the SiO release cannot be detected by MS because this compound is only stable at high temperatures and condenses on the cold walls of the device. The existence of silica at the surface of SiCN powders has been observed by XPS and TEM.[23]

The carbon monoxide evolution arises essentially from active oxidation of SiC which can be described either by the reaction (11) at 900°C, or by the reaction (12) above 1400°C.[24]

$$SiC + O_2 \longrightarrow \overrightarrow{SiO} + \overrightarrow{CO} \quad (11)$$

$$2\,SiO_2 + SiC \longrightarrow 3\,\overrightarrow{SiO} + \overrightarrow{CO} \quad (12)$$

Consequently, the results concerning the thermal stability of SiCN nanopowders under inert atmosphere indicate that the stability of SiCN29 nanopowder is better than that of SiCN35. This stability difference is confirmed by the temperature of the maximum evolution of gaseous products (N_2, N_2O) which is higher for SiCN29 (1500°C) than for SiCN35 (1100°C).

Under reactive atmosphere (N_2), the important weight gain with the evolution of carbon monoxide and nitrous oxide, observed particularly for SiCN35 nanopowder, is due to the nitriding of the powders according to the following reactions:

$$SiC_xN_yO_z + N_2 \longrightarrow Si_3N_4 + \overrightarrow{CO} + \overrightarrow{N_2O} + \overrightarrow{SiO} \quad (13)$$

$$3\,Si + 2\,N_2 \longrightarrow Si_3N_4 \quad (14)$$

$$3\,SiC + 2\,N_2 \longrightarrow Si_3N_4 + 3\,C_{(free)} \quad (15)$$

For SiCN35 nanopowder, reactions (13) and (14) are predominant because this powder is composed of a $SiC_xN_yO_z$ amorphous phase and free silicon. The SiC nitriding (15) is also possible,[25] but should be considered as a minor reaction given that amorphous phases and free silicon, less stable than crystallised SiC under nitrogen, will be preferentially nitrided. This is confirmed by XRD patterns of SiCN35 treated under nitrogen where silicon nitride appears and free silicon disappears, compared to the as-synthesized powder.

For SiCN29 nanopowder, the heat treatment under nitrogen involves a low weight gain indicating a slight nitriding. Such a phenomenon is associated with the chemical composition (high Si_3N_4 content) and the initial structure (well crystallised) of the SiCN29 powder.

According to the α (or β) Si_3N_4 content calculated from XRD patterns of heat treated powders, the nitriding leads to the preferential formation of α phase. This phenomenon has also been reported by Giorgi *et al.*[25] and could be explained by an oversaturation in nitrogen coming from the treatment atmosphere which results in the crystallization of the less ordered phase (α). Meanwhile, the β silicon nitride phase, more ordered and stable, is preferentially formed during annealing under inert atmosphere (He).

3.5.2 Reactivity of SiCN nanopowders with sintering aids

Whatever the powder, the α to β Si_3N_4 transformation rate is related to the solution–diffusion–precipitation process which is the second stage of liquid phase sintering.[26] Dissolution of SiCN nanopowders in the YSiAlON(C) liquid phase is faster than that of Si_3N_4 powder because of the small size of the SiCN particles. Thus, compared to Si_3N_4, the transformation rate is enhanced by the

small grain size of SiCN nanopowders [S_{BET} around $45\,m^2g^{-1}$ for SiCN nanopowders compared with $15\,m^2g^{-1}$ for Si_3N_4] which controls the reactivity with the liquid phase during heat treatment.

Moreover, the comparison of the reactivity of the two SiCN nanopowders with sintering aids indicates that the α to β Si_3N_4 transformation rate is increased by the presence of SiC particles. Such a phenomenon, also reported for Si_3N_4/SiC nanocomposites in previous work,[13] indicates that silicon carbide influences the precipitation step: the β Si_3N_4 phase (in fact, β SiAlON solid solution, with a very low aluminum content) should grow on SiC nanoparticles which allow a decrease of the energy barrier necessary for the precipitation of β Si_3N_4.

4 Conclusion

TG/MS study in conjunction with XRD analysis has revealed that the thermal behaviour of SiCN nanopowders depends both on the nature of the gaseous atmosphere, and on the chemical composition and structure of the starting powder.

Under inert atmosphere (He), the results provide evidence for a significant decomposition of the powders which is the more important as the degree of crystallisation and the nitrogen content decrease in the SiCN starting nanopowder. In the case of a quasi amorphous powder (SiCN35), the heat treatment under helium induces the powder crystallisation and the preferential formation of the silicon nitride β phase. The same treatment of a crystallised and Si_3N_4-rich SiCN nanopowder which is free of silicon (SiCN29) leads to a slight increase of β Si_3N_4 content and the formation of silicon.

Meanwhile, under reactive atmosphere (N_2), the quasi amorphous powder containing a small nitrogen content (SiCN35) is significantly nitrided. This nitriding reaction is accompanied by the crystallisation and the preferential formation of the silicon nitride α phase. For the crystallised powder containing a high nitrogen content (SiCN29), the nitriding process is slight. No variation between the α/β ratio of the nitrogen treated SiCN29 powder and that of the starting powder has been observed, revealing that the thermal behaviour of such a powder is close to that of a silicon nitride powder in this temperature range.

Reactivity with sintering aids (Y_2O_3, Al_2O_3) is more important for SiCN nanopowders than for Si_3N_4 UBE powder. The grain size and the chemical composition of nanopowders control the α to β Si_3N_4 phase transformation, that is to say that the small grain size and the presence of SiC induce an increase of transformation rate.

References

1. Siegel, R. W., Synthesis, structure and properties. In *Nanophase Materials*, ed. F. E. Fujita. Springer Series in Materials Science Physics of New Materials, Vol. 27, 1994, pp. 65–78.
2. Dagani, R., Nanostructured materials promise to advance range of technologies. *Science Technology*, 1992, **23**, 18–24.
3. Niihara, K., New design concept of structural ceramics–ceramic nanocomposite. *J. Cer. Soc. Jap.*, 1991, **99**(10), 974–982.
4. Ishizaki, K. and Yanai, T., Si_3N_4 grain boundary reinforcement by SiC nanocomposites. *Silicates Industriels*, 1995, **7–8**, 215–222.
5. Hirano, T., Nakahira, A. and Niihara, K., Effect of SiC particles on $\alpha - \beta$ phase transformation and mechanical properties of Si_3N_4/SiC composites. *Funtai Oyob. Fun. Yak.*, 1994, **41**(10), 1243–1248.
6. Niihara, K., Hirano, T., Nakahara, A., Ojima, K., Izaki, K. and Kawakami, T., High temperature performance of Si_3N_4–SiC composites from fine amorphous SI–C–N powder. In MRS International Meeting on Advanced Materials. Materials Research Society, 1989, 5, 107–112.
7. Wakai, F., Kodama, Y., Sakaguchi, S., Murayama, N., Izaki, K. and Niihara, K., A superplastic covalent crystal composite. *Nature*, 1990, **344**, 421–423.
8. Cauchetier, M., Croix, O., Luce, M., Baraton, M-I., Merle, T. and Quintard, P., Nanometric Si/C/N composite powders: laser synthesis and IR characterization. *J. Eur. Cer. Soc.*, 1991, **8**, 215–219.
9. Driss-Khodia, M., Gheorghiu, A., Dufour, G., Roulet, H., Sénémaud, C. and Cauchetier, M., Electronic structure of nanometric Si/C, Si/N and Si/C/N powders studied by both X-ray-photoelectron and soft-X-ray spectroscopies. *Physical Review B*, 1996, **53**(8), 4287–4293.
10. Gheorghiu, A., Sénémaud, C., Roulet, H., Dufour, G., Moreno, T., Bodeur, S., Reynaud, C., Cauchetier, M. and Luce, M., Atomic configurations and local order in laser-synthesized Si, Si–N, Si–C, and Si–C–N nanometric powders, as studied by X-ray-induced photoelectron spectroscopy and extended X-ray-absorption fine structure analysis. *J. Appl. Phys*, 1992, **71**(9), 4118–4127.
11. Ténégal, F., Flank, A-M. and Herlin, N., Short-range atomic structure description of nanometric Si/C/N powders by X-ray-absorption spectroscopy. *Physical Review B*, 1996, **54**(17), 12029–12035.
12. Gazzara, C. P. and Messier, D. R., Determination of phase content of Si_3N_4 by X-ray diffraction analysis. *Cer. Bull.*, 1977, **56**(9), 777–780.
13. Mayne, M., Bahloul-Hourlier, D., Goursat, P. and Besson, J-L., Elaboration et propriétés mécaniques de composites Si_3N_4/SiCxNy. *C.R. Acad. Sci. Paris*, **t. 320**, Série II b, 1995, 433–439.
14. Cauchetier, M., Croix, O., Herlin, N. and Luce, M., Nanocomposite Si/C/N powder production by laser–aerosol interaction. *J. Am. Cer. Soc.*, 1994, **77**(4), 993–998.
15. Moedritzer, K., Redistribution reaction. *Organomet. React.*, 1971, **2**, 1–155.
16. Bahloul, D., Pereira, M. and Gerardin, C., Pyrolysis chemistry of polysilazane precursors to silicon carbonitride—Part 1. Thermal degradation of the polymers. *J. Mater. Chem.*, 1997, **7**(1), 109–116.
17. Hasegawa, Y. and Okamura, K., Synthesis of continuous silicon carbide fiber. Part 2. Conversion of poly(-carbosilane) fiber into silicon carbide fibers. *J. Mater. Sci*, 1983, **15**, 720–728.
18. Hasegawa, Y. and Okamura, K., Synthesis of continuous silicon carbide fiber. Part 3. Pyrolysis process of polycarbosilane and structure of the products. *J. Mater. Sci*, 1983, **18**, 3633–3648.
19. Bahloul, D., Pereira, M. and Goursat, P., Preparation of silicon carbinitrides from an organosilicon polymer: II,

thermal behavior at high temperatures under argon. *J. Am. Ceram. Soc.*, 1993, **76**(5), 1163–1168.
20. Dean Batha, H. and Dow Whitney, E., Kinetics and mechanism of the thermal decomposition of Si_3N_4. *J. Am. Ceram. Soc.*, 1973, **56**(7), 365–369.
21. Sata, T. and Fujii, K., Behavior of Si_3N_4 and Si_2ON_2 in nitrogen with 10^{-10} atm of oxygen between 1100 and 1800°C. Report of the Research Laboratory of Engineering Materials, Vol. 6. Tokyo Institute of Technology, Tokyo. 1981, pp. 123–130.
22. Narushima, T., Iguchi, Y., Goto, T., Hirai, T. and Yokoyama, Y., High-temperature active oxidation of CVD- Si_3N_4 in Ar–O_2 atmosphere. *Solid State Ionics*, 1992, **53–56**, 265–269.
23. Mayne, M., Elaboration, microstructure et comportement au fluage de nanocomposites Si_3N_4/SiCN. PhD. Limoges University, France, 1997.
24. Filsinger, D. H. and Bourrie, D. B., Silica to silicon: key carbothermic reaction and kinetics. *J. Am. Ceram. Soc.*, 1990, **73**(6), 1726–1732.
25. Giorgi, R., Turttù, S., Zappa, G., Borsella, E., Botti, S., Cesile, M. C. and Martelli, S., Microstructural properties of laser synthesized Si/C/N nanoparticles. *Applied Surface Science*, 1996, **93**, 101–108.
26. Ziegler, G., Heinrich, J. and Wotting, G., Review—relationships between processing, microstructure and properties of dense reaction-bonded silicon nitride. *J. Mater. Sci.*, 1987, **22**, 3041–3086.